2011 50th IEEE Conference on Decision and Control and
European Control Conference (CDC-ECC)
Orlando, FL, USA, December 12-15, 2011

Energy-Efficient Tracking Control of Pneumatic Cylinders

Jihong Wang, *Senior Member, IEEE,* Tim Gordon

***Abstract*— Pneumatic actuators have been widely used in industry for over a hundred years. However, it is well-known that pneumatic actuators have very poor energy efficiency. Also, it is difficult to achieve accurate positioning due to the inherent nonlinearity caused by air compressibility. This paper presents recent work in developing an energy-efficient tracking control strategy for pneumatic cylinders. The pneumatic system is initially transformed into a linear system description using the nonlinear input/output feedback linearization method. Then energy efficient velocity profile is derived based on optimal control theory. A servo/tracking controller is then designed to drive the system to follow the derived new energy efficiency velocity profile. The simulation study indicates that energy consumption can be reduced by 3-5%.**

***Index Terms*— optimal control, tracking control; pneumatic actuators; nonlinear systems; feedback linearisation.**

I. Introduction

In many traditional applications, linear pneumatic actuators are chosen for motion control systems when cheap, clean, simple and safe operating conditions are available. In recent years, many reports can be found for employing pneumatic actuators to accomplish more sophisticated motion control tasks due to advances of technology ([1-6]). However, pneumatic actuators have two main drawbacks which have limited their use:

1) Inherent nonlinearities associated with compressibility of air and complex friction distributions make accurate position and velocity control extremely challenging. The advanced nonlinear control theory seems to provide a possible solution ([5][6]). But in practice, the structure of the nonlinear controller is overly complicated for real-time implementation.

2) In most cases, energy efficiency is around 20~30% and sometimes lower than 20% ([7]). Although much effort has been made ([8-12]), little significant progress has been made in the energy efficiency improvement.

The paper aims to address the above issues, in particular, for servo pneumatic actuator systems. The method proposed in the paper is based on the nonlinear input/output feedback linearization and optimal control theory. An energy-efficient velocity profile is then derived so the servo/tracking control objective is to drive the cylinder piston to follow the energy efficient profile. A design procedure is illustrated in Figure 1. The paper is organized to follow the procedure illustrated in Figure 1in a step by step manner.

The authors would like to thank the grant support from EPSRC (EP/F027265/1), Advantage West Midlands and the European Regional Development Agency for the support of Birmingham Science City Energy Efficiency & Demand Reduction project.

Jihong Wang is with the School of Engineering, the University of Warwick, Coventry CV4 7AL, UK; Tel: +44-2476466865; Fax: 0044-2476418922; E-mail: jihong.wang@warwick.ac.uk.

Tim Gordon is with the Department of Mechanical Engineering, University of Michigan, Ann Arbor, USA. Tel: +1-7347636156; Fax: +1-7347644256; E-mail: tjgordon@umich.edu

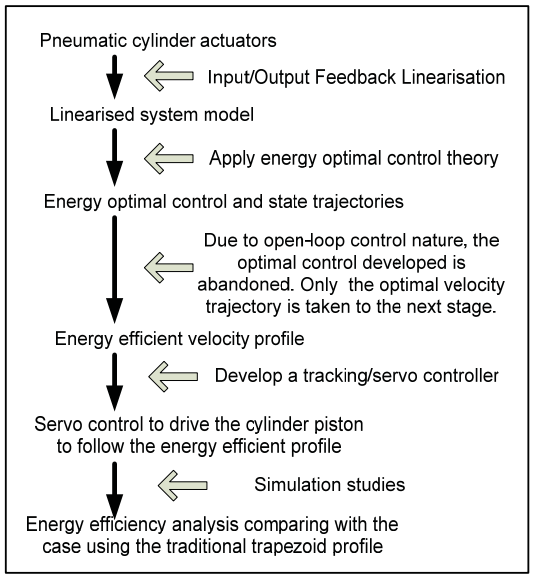

Figure 1. Flow chart for the design and analysis procedure.

II. Mathematical Model of Pneumatic Cylinders

An analysis of dynamics of a pneumatic system usually requires individual mathematical descriptions of the three component parts ([13]): (i) the valve, (ii) the actuator, and (iii) the load. The coordinate system is shown in Figure 2.

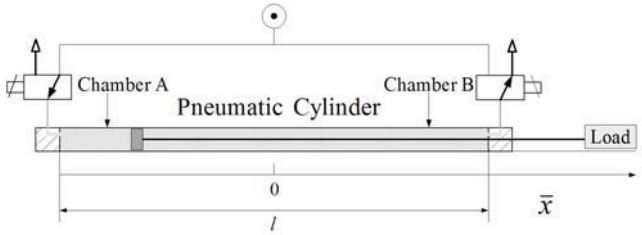

Figure 2. Co-ordinate system of a pneumatic cylinder

The following symbols are used to describe the underlying mathematical model:

a, b	Subscripts for inlet and outlet chambers respectively
A	Ram area (m^2)
C_d	Discharge coefficient
Δ	The generalized residual chamber volume

K_f Viscous frictional coefficient
k Specific heat constant
l Stroke length (m) and $\bar{x} \in (-l/2,\ l/2)$
m Mass flow rate (Kg/s)
M Payload (Kg)
P_d Down stream pressure (N/m^2)
P_e Exhaust pressure (N/m^2)
P_s Supply pressure (N/m^2)
P_u Upstream pressure (N/m^2)
R Universal gas constant (JK/Kg)
T_s Supply temperature (K)
V Volume (m^3)
w Port width (m)
$\bar{x}$ Load position (m)
$X_{a,b}$ Spool displacements of Valve A or Valve B (m)

$k = 1.4$, $T_s = 293$ K, $R = 287$JK/Kg, $P_s = 6\times10^5$ N/m^2, $P_e = 1\times10^5$ N/m^2, $C_d = 0.8$, $C_r = \left(2/[k+1]\right)^{\frac{k}{k-1}} = 0.528$, and $C_k = \sqrt{2\quad \left([k+1]/2\right)^{\frac{k+1}{k-1}}/[k-1]} = 3.864$.

With the co-ordinates illustrated in Figure 1, pneumatic cylinder actuators can be modelled as follows (for detailed analysis, see [13]):

$$\dot{x}_1 = x_2 \quad \text{(1a)}$$

$$\dot{x}_2 = [-K_f x_2 - K_{S-c}S(x_2,x_3,x_4) + A_a x_3 - A_b x_4]/M \quad \text{(1b)}$$

$$\dot{x}_3 = \frac{-k[x_3 x_2 - RT_s C_d C_0 w_a \hat{f}(x_3,P_s,P_e)u_1/A_a]}{(l/2 + x_1 + \Delta)} \quad \text{(1c)}$$

$$\dot{x}_4 = \frac{k[x_4 x_2 + RT_s C_d C_0 w_b \hat{f}(x_4,P_s,P_e)u_2/A_b]}{(l/2 - x_1 + \Delta)} \quad \text{(1d)}$$

where $x_1 = \bar{x}$, $x_2 = \dot{\bar{x}}$, $x_3 = P_a$, $x_4 = P_b$, $u_1 = X_a$ and $u_2 = X_b$. The functions in Equations (1) are defined as:

$$\widetilde{f}(p_r) = \begin{cases} 1, & P_{atm}/P < p_r \le C_r \\ C_k\left[p_r^{\frac{2}{k}} - p_r^{\frac{(k+1)}{k}}\right]^{\frac{1}{2}}, & C_r < p_r < 1. \end{cases}, \quad (2)$$

$$\hat{f}(x_3,P_s,P_e) = \begin{cases} P_s\widetilde{f}(\frac{x_3}{P_s})/\sqrt{T_s}, \text{ A : drive chamber} \\ x_3\widetilde{f}(\frac{P_e}{x_3})/\sqrt{T_a}, \text{ A : driven chamber} \end{cases} \quad (3a)$$

and

$$\hat{f}(x_4,P_s,P_e) = \begin{cases} x_4\widetilde{f}(\frac{P_e}{x_4})/\sqrt{T_b}, \text{ A : driven chamber} \\ P_s\widetilde{f}(\frac{x_4}{P_s})/\sqrt{T_a}, \text{ A : drive chamber} \end{cases} \quad (3b)$$

The term $-K_f x_2 - K_{S-c}S(x_2,x_3,x_4)$ in Equation (1b) represents the summing effects of static and dynamic friction forces in the system, where

$$K_{S-c}(x)S(\dot{x},x_3,x_4) := \begin{cases} (A_a x_3 - A_b x_4), \\ \quad \text{for } \dot{x} = 0 \text{ and } \left|A_a x_3 - A_b x_4\right| \le K_S(x_1) \\ K_c(x_1)sign(\dot{x}_2), \\ \quad \text{for } \dot{x} \ne 0 \text{ or } |A_a x_3 - A_b x_4| > K_S(x_1) \end{cases},$$

in which $K_S(x_1)$ represents position dependent static frictions and $K_c(x_1)$ represents the variable position dependent load caused by friction effects ([14-16]). Model validation can be found in [13].

I. Input-output feedback linearisation

The system described in (1) has single input and single output form, with the following mathematical structure:

$$\dot{\hat{\mathbf{x}}} = f(\hat{\mathbf{x}}) + g(\hat{\mathbf{x}})u,\ y = h(\hat{\mathbf{x}}) \quad (4)$$

where $\hat{\mathbf{x}} \in \Re^n$ is the state vector, $u \in \mathcal{R}$ represents the input, and $y \in \mathcal{R}$ is the system output. Here, in (4), f and g are C^∞ vector fields on $\Re^n$ and h is a C^∞ function on $\mathcal{R}$. The system is called static state feedback input-output linearisable by regular static state feedback and coordinate transformation, if there exists an invertible feedback, i.e.

$$u = \alpha(\hat{\mathbf{x}}) + \beta(\hat{\mathbf{x}})v \quad (5)$$

with $\frac{\partial\beta(\hat{\mathbf{x}})}{\partial\hat{\mathbf{x}}} \not\equiv 0$ and a coordinate change of

$$\mathbf{z} = \phi(\hat{\mathbf{x}}) \quad (6)$$

Under the z-coordinates and the new input v, System (4) becomes

$$\dot{\mathbf{z}}^1 = \mathbf{A}\mathbf{z}^1 + \mathbf{b}v$$
$$\dot{\mathbf{z}}^2 = f^2(\mathbf{z}^1,\mathbf{z}^2) + g^2(\mathbf{z}^1,\mathbf{z}^2)v$$
$$y = \mathbf{c}^T\mathbf{z}^1$$

where $\mathbf{A}, \mathbf{b},$ and $\mathbf{c}$ are constant matrices of proper dimensions ([17]). For a single input and single output system, if the system has a relative degree $r \le n$, the first set components of the local co-ordinate transformation can be chosen as ([17] pp141-142):

$$\left.\begin{aligned} &\phi_1(\hat{\mathbf{x}}) = h(\hat{\mathbf{x}}) \\ &\phi_2(\hat{\mathbf{x}}) = L_f h(\hat{\mathbf{x}}) \\ &\cdots \\ &\phi_r(\hat{\mathbf{x}}) = L_f{}^{r-1}h(\hat{\mathbf{x}}) \end{aligned}\right\} \quad (7)$$

and it is always possible to find n-r more functions $[\phi_{r+1}(\hat{\mathbf{x}})\ \ \phi_{r+2}(\hat{\mathbf{x}})\ \cdots\ \phi_n(\hat{\mathbf{x}})]$ such that the mapping $\phi_{r+1}(\hat{\mathbf{x}})\ \ \phi_{r+2}(\hat{\mathbf{x}})\ \cdots\ \phi_n(\hat{\mathbf{x}})$ qualifies as a local coordinate transformation in a neighbourhood of $\hat{\mathbf{x}}^0$ ([17]). Note that $[\phi_{r+1}(\hat{\mathbf{x}})\ \ \phi_{r+2}(\hat{\mathbf{x}})\ \cdots\ \phi_n(\hat{\mathbf{x}})]$ can be arbitrarily chosen and

the choice is highly dependent on individual systems. For a multi-input system, $u \in \Re^m$ represents the inputs and $g(\bar{\mathbf{x}}) \in \Re^{n\times m}$. In this case, the static state feedback has the same form as shown in (5) with $\alpha(\bar{\mathbf{x}}) \in \Re^m$, $\beta(\bar{\mathbf{x}}) \in \Re^{m\times m}$ an invertible matrix. As there is only one output, the local co-ordinate transformation can be chosen in the same way as the one used for the case of single input and single output systems.

When applying the above theory to the case of pneumatic actuator systems, for the convenience of analysis, the static friction forces are ignored initially and will be brought in as uncertainties in the later sections. The servo pneumatic actuator is driven by two three-port proportional valves so, comparing with the general formulation (4), the system takes the following form:

$$f(\mathbf{x}) = \begin{bmatrix} x_1 \\ (-K_f x_2 + A_a x_3 - A_b x_4)/M \\ -k x_3 x_2 / \{l/2 + x_1 + \Delta\} \\ -k x_4 x_2 / \{l/2 - x_1 + \Delta\} \end{bmatrix},$$

$$g(\mathbf{x}) = \begin{bmatrix} 0 \\ 0 \\ \dfrac{kRT_s C_d C_0 w \hat{f}(x_3, P_s, P_e)}{A_a(l/2 + x_1 + \Delta)} \\ -\dfrac{kRT_s C_d C_0 w \hat{f}(x_4, P_s, P_e)}{A_b(l/2 - x_1 + \Delta)} \end{bmatrix}$$

and $y = h(\mathbf{x}) = x_1$, where f and g are C^∞ vector fields on the set $\Omega \subset \Re^4$ (there are some constraints on the system variables and parameters in practice), $y = h(\mathbf{x}) \in (-l/2,\ l/2) \subset \Re$. For this system, $L_g L_f{}^\kappa h(\mathbf{x}) = 0$, for all $\kappa < 3$ and $L_g L_f{}^\kappa h(\mathbf{x}) \neq 0$ for $\kappa = 3$ ($\forall \mathbf{x}$). So the relative degree of the system is 3. Applying the general formation of mapping functions in (7), the following co-ordinates can be chosen for transformation from a nonlinear to a linear system ([13]):

$$\left.\begin{aligned} z_1 &= x_1 \\ z_2 &= x_2 \\ z_3 &= [-K_f x_2 + A_a x_3 - A_b x_4]/M \\ z_4 &= x_4 \end{aligned}\right\} \tag{8}$$

Applying the transformation (8), the pneumatic system is then transformed into:

$$\left.\begin{aligned} \dot{z}_1 &= z_2 \\ \dot{z}_2 &= z_3 \\ \dot{z}_3 &= -\frac{K_f}{M} z_3 - \frac{k(z_2 z_3 + A_b z_2 z_4/M + K_f z_2^2/M)}{l/2 + z_1 + \Delta} \\ &\quad + \frac{kRT_s C_d C_0 w_a \hat{f}(z, P_s, P_e)}{M(l/2 + z_1 + \Delta)} u_1 - \frac{A_b k z_4 z_2}{M(l/2 - z_1 + \Delta)} \\ &\quad - \frac{kRT_s C_d C_0 w_b \hat{f}(z_4, P_s, P_e)}{M(l/2 - z_1 + \Delta)} u_2 \\ \dot{z}_4 &= \frac{k z_4 z_2}{l/2 - z_1 + \Delta} + \frac{kRT_s C_d C_0 w_b \hat{f}(z_4, P_s, P_e)}{A_b(l/2 - z_1 + \Delta)} u_2 \end{aligned}\right\} \tag{9}$$

Let

$$u_1 = \frac{M(l/2 + z_1 + \Delta)}{kRT_s C_d C_0 w_a \hat{f}(z, P_s, P_e)} \left[\frac{k(z_2 z_3 + A_b z_2 z_4/M + K_f z_2^2/M)}{l/2 + z_1 + \Delta} + \frac{K_f}{M} z_3 + V_3\right] \tag{10a}$$

$$u_2 = \frac{A_b(l/2 - z_1 + \Delta)}{kRT_s C_d C_0 w_b \hat{f}(z_4, P_s, P_e)} \left[\frac{-k z_2 z_4}{l/2 - z_1 + \Delta} + V_2\right] \tag{10b}$$

and define $V_1 = V_3 - \frac{A_b}{M} V_2$. Substituting u_1 and u_2 back into (9), we have

$$\left.\begin{aligned} \dot{z}_1 &= z_2 \\ \dot{z}_2 &= z_3 \\ \dot{z}_3 &= V_1 \\ \dot{z}_4 &= V_2 \end{aligned}\right\} \tag{11}$$

So the system (11) is completely a linear system with two independent inputs V_1 and V_2.

II. Energy Optimal Control

The linearised system model can be rewritten in a matrix form as follows:

$$\dot{z} = Az + BV \tag{12}$$

where $z = [z_1 \quad z_2 \quad z_3 \quad z_4]^T$, $V = [V_1 \quad V_2]^T$, $A = \begin{bmatrix} 0 & 1 & 0 & 0 \\ 0 & 0 & 1 & 0 \\ 0 & 0 & 0 & 0 \\ 0 & 0 & 0 & 0 \end{bmatrix}$, and $B = \begin{bmatrix} 0 & 0 \\ 0 & 0 \\ 1 & 0 \\ 0 & 1 \end{bmatrix}$. The aim of energy efficient control is to derive a feedback control $V(z)$, for system (12) to minimise the following performance index:

$$J = \alpha z_3^2(T) + \int_0^T V^T V dt \tag{13}$$

where $\alpha z_3^2(T)$ means to minimize the final stage deceleration and $\int_0^T V^T V dt$ represents the integration of the control effort or the energy consumption. If the piston is assumed to move from one end to the other of the cylinder, the boundary conditions can be summarised as the piston position $z_1(0) = -l/2$, $z_1(T) = l/2$ or $z_1(0) = l/2$, $z_1(T) = -l/2$, which depends on the directions of the piston

movement, the piston velocity $z_2(0)=0$, $z_2(T)=0$, the initial air pressures in Chambers A and B are represented by $z_3(0)=z_3^0$ and $z_4(0)=z_4^0$ respectively but the final pressures $z_3(T)$ and $z_4(T)$ are unknown. To obtain the optimal control solution, the first step is to construct a Hamiltonian function - $H(z,V,t,\lambda)$ with an associated multiplier $\lambda \in R^4$ shown below ([18]):

$$H(z,V,t,\lambda)=V^TV+\lambda^T(Az+BV) \tag{14}$$

Then we have ([18]):

$$\dot{z}=\frac{\partial H}{\partial \lambda}=Az+BV \tag{15}$$

$$-\dot{\lambda}=\frac{\partial H}{\partial z}=A^T\lambda \tag{16}$$

$$0=\frac{\partial H}{\partial V}=2V+B^T\lambda \tag{17}$$

The solutions for the above equations are

$$\lambda_1=\mu_1,\quad \lambda_2=-\mu_1 t+\mu_2$$

$$\lambda_3=\mu_1 t^2/2-\mu_2 t+\mu_3,\quad \lambda_4=\mu_4$$

and

$$z_4=-\mu_4 t/2+\mu_5$$

$$z_3=-\left(\mu_1 t^3/6-\mu_2 t^2/2+\mu_3 t+\mu_6\right)/2 \tag{18}$$

$$z_2=-\left(\mu_1 t^4/24-\mu_2 t^3/6+\mu_3 t^2/2+\mu_6 t+\mu_7\right)/2$$

$$z_1=-\frac{1}{240}\mu_1 t^5+\frac{1}{48}\mu_2 t^4-\frac{1}{12}\mu_3 t^3-\frac{1}{4}\mu_6 t^2-\frac{1}{2}\mu_7 t+\mu_8$$

where $\mu_1=-\frac{1440l}{T^5}-\frac{120}{T^3}z_3(T)$, $\mu_2=\frac{-720l}{T^4}-\frac{48}{T^2}z_3(T)$,

$\mu_3=\frac{-120l}{T^3}-\frac{6}{T}z_3(T)$, $\mu_5=z_4(0)$, $\mu_4=\frac{2}{T}\left[z_4(0)-z_4(T)\right]$,

$\mu_6=0$, $\mu_7=0$, $\mu_8=-l/2$.

The optimal control with respect to the linearised system model is derived as

$$V_1=-(\mu_1 t^2/4-\mu_2 t/2+\mu_3/2)$$

$$V_2=-\mu_4/2$$

The energy efficient optimal control for the pneumatic actuator system is then obtained by substituting V_1 and V_2 into (9) which are:

$$u_1=\frac{M(l/2+z_1+\Delta)}{kRT_sC_dC_0w_a\hat{f}(z,P_s,P_e)}\left[\frac{k(z_2z_3+\frac{A_bz_2z_4+K_fz_2^2}{M})}{l/2+z_1+\Delta}+\frac{K_fz_3}{M}-(\frac{\mu_1t^2}{4}-\frac{\mu_2t}{2}+\frac{\mu_3}{2})\right] \tag{19}$$

$$u_2=\frac{A_b(l/2-z_1+\Delta)}{kRT_sC_dC_0w_b\hat{f}(z_4,P_s,P_e)}\left[\frac{-kz_2z_4}{l/2-z_1+\Delta}+\mu_4\right] \tag{20}$$

The optimal control in (19) and (20) can minimise J and in turn minimize the energy used to move the piston from one position to another. However, the energy optimal control is an open-loop control in nature so it has very limited potential to be used in practice. How can this optimal control help improve pneumatic actuator energy efficiency?

An idea of energy efficient tracking control is now proposed. Although the optimal control may not be available to be used in practice, the energy optimal velocity trajectory might be used as the servo pneumatic actuator's velocity profile. Then, the tasks for the next step will be to answer the following questions: 1) is it possible to develop a robust tracking control to follow the velocity derived using optimal control theory? 2) can energy be saved if the traditional trapezoid velocity profile is replaced by the optimal velocity profile developed in the above section?

III. Energy Optimal Tracking Control

To analyze whether the velocity trajectory derived in Section IV can be used as the optimal energy velocity profile, the analysis starts from obtaining the velocity curve through simulation study. The simulation conditions specified for the simulations are: a rodless cylinder with the stroke length of 1000 mm and the bore size of 32 mm, the supply air pressure is 6 bars and the exhaust pressure is 1 bar (assuming temperature is at 293 K), payload mass is 1 Kg, viscous frictional coefficient is 15 Ns/m, the initial piston position is at -0.5 m, initial chamber pressures are 3.5 bars for both chambers. The calculations of the new states **z** has been transformed back to the original state space of **x**. The first group of simulation results are shown in Figures 3, 4. For terminal chamber pressure fixed at 3.5 bars, twenty different initial pressures were studied, these ranging from 2.0 bars to 6.0 bars. It is found that even with different initial chamber pressures the optimal trajectories of piston position, piston velocity and acceleration actually remain the same. The obtained analytic solutions of the energy efficient optimal control problem can explain why the initial and terminal chamber pressures do not affect the optimal trajectories. From the equations (18), we have

$$z_2=\left(30l/T^5\right)t^4-\left(60l/T^4\right)t^3+\left(30l/T^3\right)t^2 \tag{21}$$

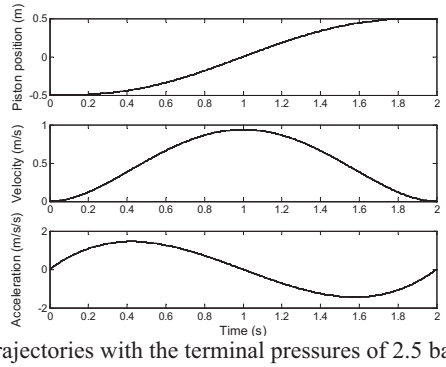

Figure 3. Trajectories with the terminal pressures of 2.5 bars

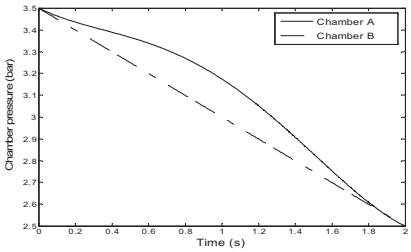

Figure 4. Chamber pressure with terminal pressures of 2.5 bars

Reference [18] reported that the servo pneumatic system uses less compressed air when a "sine" wave shape piston velocity profile was adopted comparing with the situation of using traditional trapezoidal and parabolic shape velocity profiles. The optimal and sine wave shape of profiles are illustrated in Figure 5.

From Figure 5, the sinusoidal profile is very close to the energy efficient optimal profile obtained above. As stated, it is impossible to directly apply the optimal control derived from the energy optimal control theory as it is an open-loop control. The idea here is to use the energy efficient velocity trajectory as the desired velocity profile for the servo pneumatic actuator. That is, the energy optimal velocity profile replaces the common trapezoidal profile. The next step is to develop a tracking control to drive the piston of the cylinder to follow the energy efficient profile.

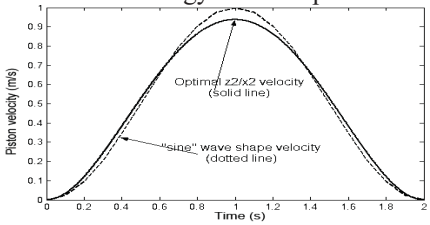

Figure 5. Comparing with a sine wave profile

With the same state variable transformation specified in (8), we choose the input/output feedback below:

$$u_1 = \frac{1}{\psi(\bar{\mathbf{z}})}\left[\frac{k(\bar{z}_2\bar{z}_3 + K_f\bar{z}_2^2/M)}{l/2+\bar{z}_1+\Delta} + \frac{A_b k(l+2\Delta)\bar{z}_2\bar{z}_4}{(l/2+\Delta)^2-\bar{z}_1^2} + V\right]$$

and set $\eta(\mathbf{z}) = \frac{1}{\psi(\bar{\mathbf{z}})}\frac{kRT_sC_dC_0w_b\hat{f}(\bar{z}_4,P_s,P_e)}{A_b(l/2-\bar{z}_1+\Delta)}$. Substituting u_1 into (9), the following can be derived

$$\begin{aligned}\dot{\bar{z}}_1 &= \bar{z}_2\\ \dot{\bar{z}}_2 &= \bar{z}_3\\ \dot{\bar{z}}_3 &= -K_f\bar{z}_3/M + V\end{aligned} \tag{22}$$

and

$$\dot{\bar{z}}_4 = \frac{k\bar{z}_4\bar{z}_2}{l/2-\bar{z}_1+\Delta} - \eta(\bar{\mathbf{z}})k\bar{z}_2\left[\frac{\bar{z}_3+K_f\bar{z}_2/M}{l/2+\bar{z}_1+\Delta} + \frac{A_b(l+2\Delta)\bar{z}_4}{(l/2+\Delta)^2-\bar{z}_1^2} + V\right]$$

$y = \bar{z}_1$. Subsystem (22) is linear with respect to $\bar{\mathbf{z}}$ and V and the input/output map of the system (22) is linear as well. The linearised subsystem (22) can be rewritten in a matrix format as follows:

$$\dot{\bar{\mathbf{z}}} = \mathbf{A_1}\bar{\mathbf{z}} + \mathbf{B_1}\mathbf{V}, \tag{23}$$

where $\bar{\mathbf{z}} = \begin{bmatrix}\bar{z}_1\\ \bar{z}_2\\ \bar{z}_3\end{bmatrix}$, $\mathbf{A_1} = \begin{bmatrix}0 & 1 & 0\\ 0 & 0 & 1\\ 0 & 0 & -K_f/M\end{bmatrix}$, and $\mathbf{B_1} = \begin{bmatrix}0\\ 0\\ 1\end{bmatrix}$.

For this tracking problem, suppose that the system output $\bar{z}_1$ is required to accurately follow the trajectory $\theta_1(t)$. As $(\mathbf{A_1},\mathbf{B_1})$ is a controllable pair, $\theta_1(t)$ can be normally generated by the same structured linear system as (21). Let $\boldsymbol{\theta} = [\theta_1 \quad \theta_2 \quad \theta_3]^T$, then

$$\begin{bmatrix}\dot{\theta}_1\\ \dot{\theta}_2\\ \dot{\theta}_3\end{bmatrix} = \begin{bmatrix}0 & 1 & 0\\ 0 & 0 & 1\\ 0 & 0 & -K_f/M\end{bmatrix}\begin{bmatrix}\theta_1\\ \theta_2\\ \theta_3\end{bmatrix} + \begin{bmatrix}0\\ 0\\ 1\end{bmatrix}\omega(t) \tag{24}$$

From (18), we have

$$\begin{bmatrix}\dot{\theta}_1\\ \dot{\theta}_2\\ \dot{\theta}_3\end{bmatrix} = \begin{bmatrix}\left(\frac{30l}{T^5}\right)t^4 - \left(\frac{60l}{T^4}\right)t^3 + \left(\frac{30l}{T^3}\right)t^2\\ 4\left(\frac{30l}{T^5}\right)t^3 - 3\left(\frac{60l}{T^4}\right)t^2 + 2\left(\frac{30l}{T^3}\right)t\\ 12\left(\frac{30l}{T^5}\right)t^2 - 6\left(\frac{60l}{T^4}\right)t + 2\left(\frac{30l}{T^3}\right)\end{bmatrix} \tag{25}$$

where $\omega(t)$ is an external input which will be designed to generate the desired trajectory $\theta_1(t)$, which is:

$$\omega(t) = \frac{60l}{T^3}\left[\frac{2}{T^2}\frac{K_f}{M}t^3 - \frac{3}{T}\left(\frac{K_f}{M}-\frac{2}{T}\right)t^2 + \left(\frac{K_f}{M}-\frac{6}{T}\right)t + 1\right].$$

Together with (12), the tracking problem is converted into an asymptotic stability problem. Let $e(t) = \theta(t) - \bar{z}(t)$, so

$$\dot{\mathbf{e}} = \dot{\boldsymbol{\theta}} - \dot{\bar{\mathbf{z}}} = \mathbf{A_1}(\boldsymbol{\theta}-\bar{\mathbf{z}}) + \mathbf{B_1}(V-\omega) = \mathbf{A_1}\mathbf{e} + \mathbf{B_1}(V-\omega)$$

A feedback controller can be developed to drive the error state $\mathbf{e}(t)$ to zero. The controller can have the structure

$$V = -\mathbf{K}\mathbf{e} + \omega,$$

where $\mathbf{K} = [K_1 \quad K_2 \quad K_3]$. The closed-loop system is then written as $\dot{\mathbf{e}} = (\mathbf{A_1} - \mathbf{B_1}\mathbf{K})\mathbf{e}$. If the feedback control can be designed to guarantee that $\sigma(\mathbf{A_1} - \mathbf{B_1}\mathbf{K}) \in C^-$, the tracking error $\mathbf{e}(t)$ will eventually approach to zero within a finite time period. Substituting the tracking control V back to the original system control u, the following is obtained:

$$\begin{aligned}u_1^{(1)} = {} & \frac{k(\bar{z}_2\bar{z}_3 + K_f\bar{z}_2^2/M)}{\psi(\bar{\mathbf{z}})(l/2+\bar{z}_1+\Delta)} + \frac{A_b k(l+2\Delta)\bar{z}_2\bar{z}_4}{\psi(\bar{\mathbf{z}})[(l/2+\Delta)^2-\bar{z}_1^2]}\\ & + [K_1(\theta_1-\bar{z}_1) + K_2(\theta_2-\bar{z}_2) + K_3(\theta_3-\bar{z}_3) + \omega]/\psi(\bar{\mathbf{z}})\end{aligned}$$

By transforming $\mathbf{z}$ back to the original system variables $\mathbf{x}$, the final feedback control $u_1(x)$ is obtained.

Next we determine whether the compressed air used can be reduced adopting the new velocity profile. A simulation study has been conducted to implement the tracking control strategy with the energy optimal velocity profile. The integration of the compressed air mass flow timing the pressure is calculated through the simulation which represents the energy consumption level. To analyse energy efficiency, a compressed air consumption index (CACI) is defined by

$$\text{CACI} = \int_{t_0}^{t_T} \text{air mass flow} \times \text{pressure}\, dt, \tag{26}$$

where the inlet port air mass flow and air pressure are used. The more air that is used, and the higher pressure at which it is delivered, the more energy is consumed. So we hope the CACI can be reduced with the strategy proposed in this paper. Applying orifice theory, the mass flow rate can be

calculated by ([11][12][14]): $\dot{m}_{air} = C_d C_0 w_a \hat{f}(x_3, P_s, P_e)u$ at the inlet port. So CACI can be calculated by

$$\text{CACI} = \int_{t_0}^{t_T} x_3(t) C_d C_0 w_a \hat{f}(x_3, P_s, P_e) u dt \qquad (27)$$

The simulation study has been carried out using the same control strategy with two different profiles. The simulation results are shown in Figures 6, 7. The results show that the velocity tracking accuracy is highly satisfactory in both cases. Figure 8 is comparesCACI for the energy efficient and traditional trapezoid velocity profiles. When zooming into the final index values, it can be found that the CACI for trapezoid profile is 2020.8 and for energy efficient profile is 1943.6. Fractional reduction is around 5% reduction in energy used when the energy-efficient profile is adopted. The simulation study was extended to many other cases including the cases with different stroke lengths, bore sizes, initial chamber pressures etc. All cases show a similar 3-5% energy saving from the new energy efficient velocity profile consistently.

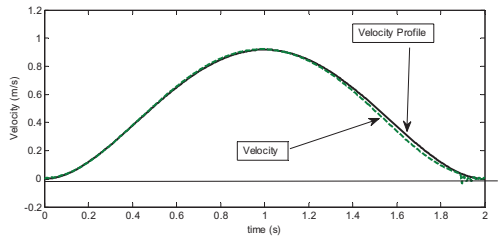

Figure 6. Velocity using energy efficient velocity profile

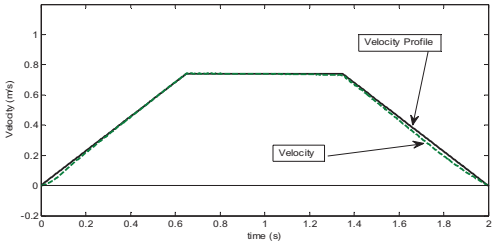

Figure 7. Velocity using trapeziod velocity profile

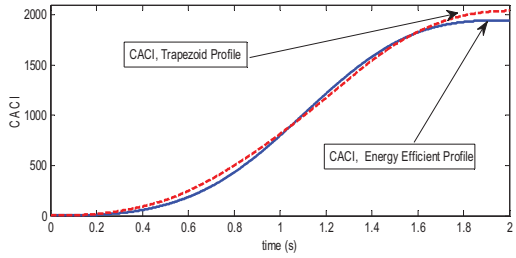

Figure 8. CACI curves for both velocity profiles

IV. Conclusion and Discussion

An energy-efficient pneumatic servo/tracking control strategy is reported in this paper. The two main advantages of the method are: 1) improvement in energy efficiency; 2) satisfactory tracking accuracy. While 3-5% may look like a very small saving, the net result can be highly significant as pneumatic actuators are widely used in industry; the cumulative benefit available should not be ignored. Importantly, adopting this method only requires the velocity profile to be changed, so it is easy to modify the software without any hardware investment. This will be very cost effective in practice. The formula to form the velocity profile is a function of the stroke length and the time interval for completing the piston movement. Therefore, it is easy to derive the velocity profile for different operation conditions. The experimental test is on going in the authors' research laboratory.

References

[1] B.W. McDonell and J.E. Bobrow, "Adaptive tracking control of an air powered robot actuator", *ASME journal of Dynamic Systems, Measurement and Control*, 1993; 115:427-433.

[2] D. Ben-Dov and S.E. Salcudean, "A force-controlled pneumatic actuator", *IEEE Transactions on Robotics and Automation*, 1995; 11:906-911.

[3] S. Drakunov, G.D. Hanchin, W.C. Su and U. Ozguner, "Nonlinear control of a rodless pneumatic servoactuator, or sliding modes versus Coulomb friction", *Actumatica*, 1997; 33:1401-1408.

[4] R.B. Van Varseveld and G.M. Bone, "Accurate position control of a pneumatic actuator using on/off solenoid valves", *IEEE/ASME Transactions on Mechatronics*, 1997; 2:195-204.

[5] Z.H. Rao and G.M. Bone, "Nonlinear modeling and control of servo pneumatic actuators", *IEEE Transactions on Control Systems*, 2008; 16:562-569.

[6] E. Richer, and Y. Hurmuzlu, "A high performance pneumatic force actuator system: Part II—nonlinear controller design", *ASME Trans. Journal of Dynamic Systems Measurement and Control*, 2000b; 122: 426-434.

[7] M.L Cai, T. Kagawa, "Energy consumption assessment of pneumatic actuating systems including compressor", *IMechE*, pp381-380, C591/03302001, 2001.

[8] K.A. Al-Dakkan, M. Goldfarb, E.J. Barth, "Energy saving control for pneumatic servo systems", IEEE/ASME International Conference on Advanced Intelligent Mechatronics, 284-289, 20-24 July 2003.

[9] X.G. Shen, M. Goldfardb, "Energy Saving in Pneumatic Servo Control Utilizing Interchamber Cross-Flow", ASME J. Dyn. Sys., Meas., Control , Vol. 129, No.3, pp303-311, 2007.

[10] A.M. Yang, J.S. Pu, C.B. Wong, P.R. Moore, "By-pass valve control to improve energy efficiency of pneumatic drive system", Control Engineering Practice, Vol. 17, No.6, pp623-628, 2009.

[11] J. Wang, L. Yang, X. Luo, S. Mangan, J.W. Derby, "Mathematical modelling study of scroll air motors and energy efficiency analysis - Part I", *IEEE/ASME Trans. on Mechatronics*, Vol. 16, No. 1, pp 112-121, 2011.

[12] J. Wang, X. Luo, L. Yang, L Shpanin, S. Mangan, J.W. Derby, "Mathematical modelling study of scroll air motors and energy efficiency analysis - Part II", *IEEE/ASME Trans. on Mechatronics*, Vol. 16, No. 1. pp122- 132, 2011.

[13] J. Wang, U. Kotta, U., J. Ke, "Tracking control of nonlinear pneumatic actuator systems using static state feedback linearisation of input/output map", *Proc. of Estonian Acad. Sci. Phys. Math.*, Vol.56, pp47-66, 2007.

[14] N. Jia, J. Wang, K. Nuttall, J.L. Wei, H.M. Xu, H.M., M. Wyszynski, J. Qiao, and M. Richardson, "HCCI engine modelling for real-time implementation and control development", *IEEE/ASME Transactions on Mechatronics*, Vol.12, pp581-589, 2007.

[15] S. Armstrong-Helouvry, P. Dupont, and C. Canudas De Wit, "A survey of model, analysis tool and compensation methodes for the control of machines with friction", *Automatica*, 1994; 30:1083-1183.

[16] J.L. Wei, J. Wang, Q.H. Wu, "Development of a multi-segment coal mill model using an evolutionary computation technique", *IEEE Transactions on Energy Conversion*, Vol. 22. pp718-727, 2007.

[17] A. Isidori, *Nonlinear Control Systems*, 3rd Edition, Springer-Verlag London, 1995.

[18] J. Ke, J. Wang, L. Yang, N. Jia, and Q.H. Wu, "Energy Efficiency Analysis and Optimal Control of Servo Pneumatic Cylinders", *IEEE Conference on Control Applications*, Canada, August, 2005.